

Localization of Two-Component Bose-Einstein Condensates in Optical Lattices

Elena A. Ostrovskaya and Yuri S. Kivshar

Nonlinear Physics Group and ARC Centre of Excellence for Quantum-Atom Optics, Research School of Physical Sciences and Engineering, Australian National University, Canberra ACT 0200, Australia

(Received 5 September 2003; published 7 May 2004)

We study nonlinear localization of a two-component Bose-Einstein condensate (BEC) in a one-dimensional optical lattice. Our theory shows that spin-dependent optical lattices can be used to effectively manipulate the nonlinear interactions between the BEC components, and to observe composite localized states of a BEC in both bands and gaps of the matter-wave spectrum.

DOI: 10.1103/PhysRevLett.92.180405

PACS numbers: 03.75.Lm, 03.75.Mn

Current experiments on Bose-Einstein condensates (BECs) in optical lattices, including nonlinear Landau-Zener tunneling [1], modulational instability of Bloch waves [2], and diffraction compensation [3,4], indicate growing interest in nonlinear dynamics of coherent matter waves in tunable periodic potentials. The interdisciplinary nature of these studies is highlighted by strong parallels [5] drawn between nonlinear optics of ultracold atoms in lattices and behavior of optical waves in periodic nonlinear photonic structures, where instability and localization phenomena have been well explored [6]. Akin to optical waves in periodic photonic structures, such as waveguide arrays and photonic crystals, coherent matter waves in optical lattices display a band-gap spectrum, which modifies diffraction properties of atomic wave packets [7]. The coexistence of both normal and anomalous diffraction regimes was predicted to lead to nonlinear localization of a condensate with either attractive or repulsive interactions in the gaps of a linear Bloch-wave spectrum [8]. Bright *gap solitons* of a *repulsive* BEC were recently observed [9].

Most of the studies of coherent matter waves in optical lattices are concerned with single-component BECs. However, condensate mixtures can display many novel physical effects not found in single-species BECs [10]. Experiments on spin-dependent optical lattices [11] have shown that a two-component BEC composed of two hyperfine states of the same atomic species can be effectively and coherently manipulated in an optical lattice. Recently, mean-field analysis of periodic Bloch states of a multicomponent BEC in a lattice [12,13] has revealed that the modulational instability of excited periodic states can potentially lead to the formation of multicomponent localized states (solitons) [13].

In this Letter, we consider nonlinear localization of a two-component BEC and formation of composite atomic solitons in an optical lattice. We show that an optical lattice can be used to *modify the effective nonlinear interactions both within and between the BEC components*, without the Feshbach resonance manipulation of scattering lengths. Consequently, novel types of nonlinear localization of coherent matter waves can be

achieved both in gaps and bands of the linear Bloch-wave spectrum. In particular, when one of the BEC components is in a periodic Bloch (band) state, the second component exhibits effective periodic potential induced by the mean-field of the Bloch-wave, and can be localized within the induced gap. As a result, localization of a BEC in a *self-induced lattice* can occur in the form of a two-component “band-gap” soliton.

Localization of the two-component BEC, assisted by manipulation of effective nonlinear interactions in an optical lattice, can be explored in the current BEC experiments. However, our theory has much wider applicability. For instance, it can be applied to the physics of two-component light fields in photonic lattices [6], where the possibility of *intergap* localization of multicomponent coherent light has already been suggested [14]. Moreover, the BEC localization in a Bloch-wave-induced periodic potential discussed here can be linked to localization processes in a wide range of optical [15] and solid state [16] systems exhibiting nonlinear *self-modulation*.

We model the dynamics of a two-component BEC with *repulsive* interactions by the mean-field equations for the wave functions of the condensate components $|a\rangle$ and $|b\rangle$:

$$i\frac{\partial}{\partial t}\begin{pmatrix} \Psi_a \\ \Psi_b \end{pmatrix} = \begin{pmatrix} \hat{L}_a & \hat{L}_{ab} \\ \hat{L}_{ab}^* & \hat{L}_b \end{pmatrix} \begin{pmatrix} \Psi_a \\ \Psi_b \end{pmatrix}, \quad (1)$$

where $\hat{L}_n = -\partial^2/\partial x^2 + V_n(x) + g_{nn}|\Psi_n|^2$, and $\hat{L}_{ab} = g_{ab}\Psi_a\Psi_b^*$. We assume that the two BEC components can exhibit different potentials, namely: $V_a(x) = V_0\sin^2(k_L x)$ and $V_b(x) = V_0\sin^2(k_L x + \theta)$, which can be shifted relative to each other, e.g., by varying the polarization angle in the case of a spin-dependent lattice [11]. The lattice potentials are less constrained than those realized in [11], to enable treatment of two different atomic species [17] that can be manipulated independently. The one-dimensional model (1) is derived for strongly anisotropic BEC clouds with the tight confinement directions transverse to that of the lattice [8]. It is made dimensionless by adopting the units of length $x_L = k_L^{-1}$, energy $E_R = \hbar^2 k_L^2/2m$, and time $\omega_L^{-1} = \hbar/E_R$.

The stationary states of the wave function of the n th BEC component are found as $\Psi_n(x, t) = \psi_n(x) \times \exp(-i\mu_n t)$, where μ_n is the chemical potential normalized by E_R . Without the repulsive mean-field interactions, the ground and excited states of each of the BEC components are periodic matter waves: $\psi_n = \phi_n(x) \exp(ikx)$, where the lattice momentum k lies within a Brillouin zone. The periodicity of the lattice leads to the band-gap structure of the spectrum $\mu_n(k)$. At the j th edge of the Brillouin zone $\mu_n \equiv \mu_n^{(j)}$, the wave function $\phi_n^{(j)}(x) = \phi_n^{(j)}(x + \pi/k_L)$ is a periodic Bloch state. Bloch-wave spectrum in the reduced-zone representation ($|k| < 1$) is shown schematically in Fig. 1.

A BEC wave packet, located in the k space near the j th band edge, can be described as a corresponding Bloch wave, dressed by a slowly varying (in x) envelope, $\Psi_n(x, t; \mu_n^{(j)}) = \Phi_n(x, t) \phi_n^{(j)}(x)$. For the two components $|a\rangle$ and $|b\rangle$ positioned at the band edges i and j , respectively, the envelope equations [14] take the form

$$\begin{aligned} -i \frac{\partial \Phi_a}{\partial t} &= \left[D_a^{(i)} \frac{\partial^2}{\partial x^2} - \tilde{g}_{aa}^{(ii)} |\Phi_a|^2 - \tilde{g}_{ab}^{(ij)} |\Phi_b|^2 \right] \Phi_a, \\ -i \frac{\partial \Phi_b}{\partial t} &= \left[D_b^{(j)} \frac{\partial^2}{\partial x^2} - \tilde{g}_{bb}^{(jj)} |\Phi_b|^2 - \tilde{g}_{ba}^{(ji)} |\Phi_a|^2 \right] \Phi_b, \end{aligned} \quad (2)$$

where the effective diffraction of the wave packet is defined by the curvature of the corresponding band edge, $D_{a,b}^{(i,j)} = (\partial^2 \mu_{a,b} / \partial k^2)_{\mu_{a,b} = \mu_{a,b}^{(i,j)}}$. The interaction coefficients depend on the overlap of the Bloch states at the band edges: $\tilde{g}_{ab}^{(ij)} = g_{ab}^{(ij)} \int |\phi_a^{(i)} \phi_b^{(j)}|^2 dx$. Hence, the relative displacement of the spin-dependent lattice potentials can *enhance or dampen* the cross-component nonlinear interactions without changing the effective diffraction, which introduces a new control parameter into the system. Moreover, Eqs. (2) and their complex conjugate form are equivalent, so the case of anomalous diffraction ($D_n < 0$) [7] translates into the more intuitive normal diffraction form, by changing *signs* of the effective nonlinear coefficients \tilde{g} .

Equations (2) predict *three regimes of the effective nonlinear interactions* that can be realized for two-component BECs in a lattice by appropriate preparation of the BEC wave packets relative to the band structure, as shown in Figs. 1(a)–1(c). Experimental preparation of the wave packets with a given k involves moving the optical lattice relative to the condensate [3,18]; higher bands can be populated by phase or amplitude modulations of the lattice [18]. Below we consider only the two lowest bands, $B1$ ($\mu^{(1)}|_{k=0} \leq \mu \leq \mu^{(2)}|_{k=1}$) and $B2$ ($\mu^{(3)}|_{k=1} \leq \mu \leq \mu^{(4)}|_{k=0}$).

Attractive-attractive interaction regime [Fig. 1(a)] can be realized when $\tilde{g}_{aa,bb}, \tilde{g}_{ab,ba} < 0$, $|\tilde{g}_{aa}| = |\tilde{g}_{bb}| = |\tilde{g}_{ab}| = |\tilde{g}_{ba}| \equiv \tilde{g}$. In this regime, near the band edge $\mu = \mu^{(2)}|_{k=1}$ both condensate components exhibit anomalous diffraction, and therefore can exhibit self-focusing in the form of *two-component bright gap solitons*. Equations (2) take the form of the integrable

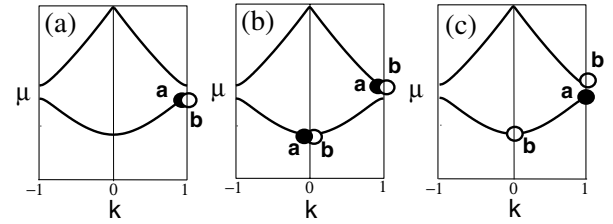


FIG. 1. Schematics of the chemical potential vs momentum of the BEC components, relative to the lattice band-gap structure, necessary to achieve the (a) attractive-attractive, (b) repulsive-repulsive, and (c) repulsive-attractive effective nonlinear interactions. In (b) and (c), for a given location of the $|a\rangle$ component either of the $|b\rangle$ states can be chosen.

Manakov system, well studied in the context of nonlinear optics (see, e.g., [19]). According to Eq. (2), both localized components can be treated as ground states of the same effective potential $V_{a,b}^{\text{eff}} = \tilde{g}(|\Phi_a|^2 + |\Phi_b|^2)$; they have equal chemical potentials $\mu_a = \mu_b$ and widths, i.e., $\Phi_a(x) = \Phi_0(x) \cos \alpha$, $\Phi_b(x) = \Phi_0(x) \sin \alpha$, where $\Phi_0(x) = \sqrt{2\mu_a/\tilde{g}_{aa}} \text{sech}(\sqrt{\mu_a}x)$, and α is arbitrary.

The existence domain for two-component solutions in the parameter space $\{\mu_a, \mu_b\}$ can also be calculated using Eqs. (1). Assuming that the atomic populations of the two-component are largely dissimilar (e.g., $\psi_a^2 \gg \psi_b^2$), one can decouple Eqs. (1) and find, numerically, spatial profiles of stationary gap solitons of the larger component, $\psi_a(x; \mu_a)$, in the entire gap $\mu_a^{(2)} \leq \mu_a \leq \mu_a^{(3)}$. The low-density second component, $|b\rangle$, then exhibits an *effective potential* $V_b^{\text{eff}} = V_b(x) + g_{ab}\psi_a^2$, due to both the optical lattice *and* mean-field interaction with the $|a\rangle$ component (the self-contribution of $|b\rangle$ to V_b^{eff} is negligible). The cutoff value $\mu_b^0(\mu_a)$ for the first bound state of the condensate wave function ψ_b in the effective potential V_b^{eff} defines the lower boundary of the existence domain for two-component localized states; the upper boundary is $\mu_b = \mu_a$. Effective potential analysis of Eqs. (1) confirms the prediction of Eqs. (2) that, in the case of equal effective interaction coefficients, the boundaries of the existence domain coincide on the line $\mu_b = \mu_a$ (see Fig. 2). This degeneracy can be lifted by shifting the lattices relative to each other. The shift unbalances the interaction coefficients so that $\tilde{g}_{ab}/\tilde{g}_{aa} > 1$, which, according to the envelope theory, yields the new cutoff values for the ψ_b modes, $\mu_b^0 = (\mu_a/4)(1 - \sqrt{1 + 8\tilde{g}_{ab}/\tilde{g}_{aa}})^2 > \mu_a$. The boundaries of the significantly expanded existence domain found by the effective potential analysis of Eqs. (1), with $\theta = \pi/4$, are shown in Fig. 2 by dashed lines. In a two-component state, each of the BEC components induces an effective potential for the other, thus the existence domain for a composite gap soliton always has two boundaries defined by the cutoff lines $\mu_b^0(\mu_a)$ and $\mu_a^0(\mu_b)$ (see Fig. 2). We note that the effective potential analysis described above is equivalent to the *linear waveguiding approach* which is widely used in the theory of multicomponent optical solitons [20].

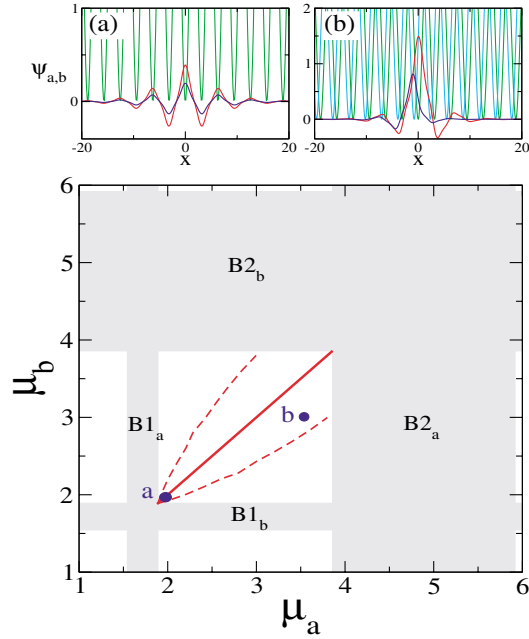


FIG. 2 (color online). Existence domain for the bright-bright atomic gap solitons in the $\{\mu_a, \mu_b\}$ plane ($V_0 = 4$). Shaded: two lowest Bloch bands $B1_{a,b}$ and $B2_{a,b}$ exhibited by the condensate components $|a\rangle$ and $|b\rangle$. Solid: existence line $\mu_a = \mu_b$ predicted by the envelope theory and effective potential calculations for $\theta = 0$. Dashed: borders of the existence domain for $\theta = \pi/4$. Top panels: condensate wave functions at the marked points, found by solving time-independent Eqs. (1). Lattice potentials are shown by dotted/green lines.

A *repulsive-repulsive* regime [Fig. 1(b)] can be achieved when $\tilde{g}_{aa,bb}, \tilde{g}_{ab,ba} > 0$, $|\tilde{g}_{ab}| = |\tilde{g}_{ba}|$, and the wave packets are located either at the same, $|\tilde{g}_{aa}| = |\tilde{g}_{bb}|$, or different, $|\tilde{g}_{aa}| \neq |\tilde{g}_{bb}|$, band edges. Let us first consider the BEC wave packet located at the edge of the second band ($B2_a$), $\mu_a = \mu_a^{(3)}|_{k=1}$. It experiences normal diffraction and can support a *dark soliton* with the envelope $\Phi_a(x) = \sqrt{\mu_a/\tilde{g}_{aa}} \tanh(\sqrt{\mu_a/2}x)$, imprinted onto the extended background of a Bloch-wave $\phi_a^{(3)}(x)$ [21]. Such a dark state with a zero group velocity can exist within the entire band, and can be created experimentally by a phase-imprinting technique. In a two-component BEC, the Bloch state in $|a\rangle$ component induces a periodic potential for the $|b\rangle$ component which acts together with the potential of the optical lattice. As a result, the band-gap structure of the Bloch-wave spectrum for the $|b\rangle$ component is significantly modified. The original bands are shifted, so that the edge of the second band $\mu_b^{(3)}$ coincides with the chemical potential of the *nonlinear* Bloch state $\phi_a^{(3)}$ (see Fig. 3). The remarkable effect of the condensate-induced lattice potential is that the $|b\rangle$ component can now be spatially localized in every gap of the *induced band-gap structure* in the form of a *bright gap soliton*. The existence domains for the coupled states calculated using the effective potential approach, lie entirely *within the original bands* $B1$ and $B2$. This type of localization could have a dramatic experimental

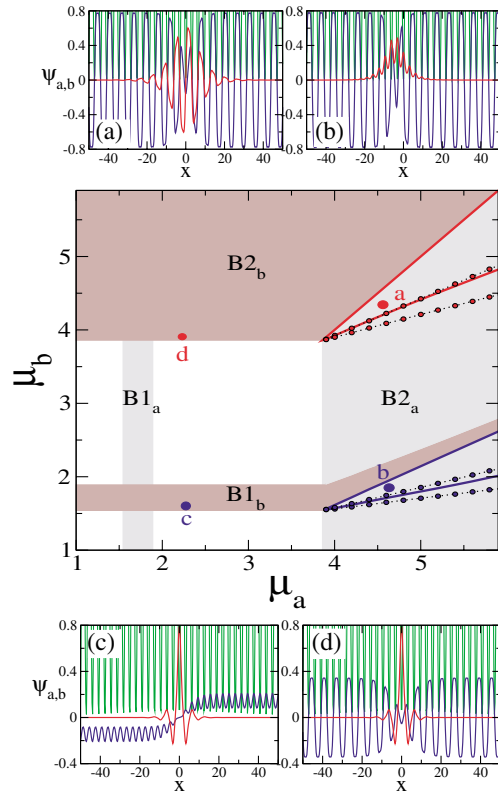


FIG. 3 (color online). Existence domains for the dark-bright atomic solitons ($V_0 = 4$). Shaded: two lowest Bloch bands $B1_{a,b}$ and $B2_{a,b}$ exhibited by the condensate components $|a\rangle$ and $|b\rangle$. Solid: borders of the existence domains in repulsive-repulsive regime for $\theta = 0$. Dotted: borders of the existence domains for $\theta = \pi/4$. Top (bottom) panels: condensate wave functions in the repulsive-repulsive (attractive-repulsive) regime at the marked points, found by solving the time-independent Eqs. (1).

manifestation, whereby formation of a bright soliton in one of the BEC components can be achieved by *phase imprinting onto the Bloch state of the complementary component* in the spectral band. This effect can be observed when both components are located either at the same or the opposite band edges [Fig. 1(b)], but always in the normal diffraction regime, where the localization of a single-component repulsive BEC in the form of a bright soliton is impossible. Therefore, although the dark-bright state can be dynamically stable [see Figs. 4(a) and 4(c)], decoupling of the BEC components leads to rapid spread of the bright state, proportional to its mean-field energy [Figs. 4(b) and 4(d)].

Dark-bright solitons supported by repulsive nonlinearity have been previously discussed in the context of nonlinear optics [19] and BEC in a harmonic potential [22]. The striking difference between the dark-bright localized states in the optical lattice and dark-bright BEC solitons in a harmonic potential is that the bright component in the lattice is localized in the gaps of the *induced band-gap structure*. This creates multiple existence domains for the dark-bright state that are adjacent to the *edges of the*

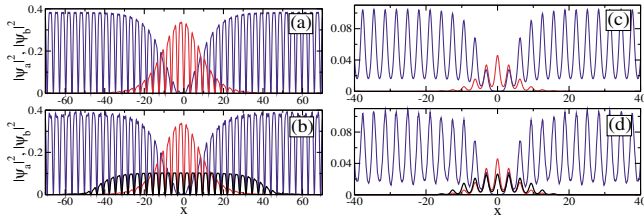


FIG. 4 (color online). Temporal evolution of a dark-bright localized state in the repulsive-repulsive regime obtained by solving Eqs. (1) with both components initially within (a),(b) the second band, at $\mu_a = 4.2$, $\mu_b = 4.18$, and (c),(d) the first band at $\mu_a = 1.62$, $\mu_b = 1.6$. Shown are (a),(c) initial spatial density profiles and (b),(d) profiles of the coupled state and (bold) a spreading bright component decoupled from the dark one at (b) $t = 1.35$ ms and (d) $t = 2.7$ ms. Note the slower expansion for the lower density state (c).

induced bands. In contrast to the case of bright-bright gap solitons, these existence domains shrink (dotted lines in Fig. 3) when $\theta \neq 0$. Another feature of the dark-bright localized states is their *inhibited mobility* across the lattice, which affects their interaction properties.

Repulsive-attractive regime [Fig. 1(c)] can be accessed when $\tilde{g}_{aa}, \tilde{g}_{ab} < 0$, $\tilde{g}_{bb}, \tilde{g}_{ba} > 0$, $|\tilde{g}_{ab}| = |\tilde{g}_{ba}|$, and $|\tilde{g}_{aa}| \neq |\tilde{g}_{bb}|$. In the absence of optical lattice, this type of interactions could be explored only for a mixture of BECs with the opposite signs of the scattering lengths. Within the lattice, the condensate wave packets should not be both prepared at the same band edge, which can pose an experimental challenge. In this regime, the envelope Eqs. (2) predict the existence of “normal” and “reverse” pairs of dark-bright solitons [20]. In the normal case, a dark soliton on the Bloch-wave background in the normal diffraction regime (e.g., at $\mu_a \geq \mu_a^{(3)}$) is coupled to a bright gap state in the anomalous diffraction regime (e.g., at $\mu_b \geq \mu_b^{(2)}$). Both components can exist independently as dynamically stable localized states, and the coupling is achieved for $\tilde{g}_{ab}^2 < |\tilde{g}_{aa}\tilde{g}_{bb}|$. Typical examples of condensate wave functions in this regime are shown in Fig. 3(c) and 3(d). The bright localized component $|a\rangle$ exists in the entire gap, whereas the dark $|b\rangle$ component forms a coupled state only in the vicinity of the band edge. The composite state is stabilized in the lattice but is unstable with respect to the mutual displacement of its constituents [20] in the lattice-free case.

Finally, we estimate the typical soliton parameters, assuming the spinor BEC of ^{87}Rb , an optical lattice with $\approx 0.4 \mu\text{m}$ spacing [11], and the atomic clouds aspect ratio of 10. We are interested in the case of relatively shallow optical lattices, with $V_0 < 5E_R$, and the chemical potentials $\mu_{a,b} \leq V_0$ (see Figs. 2 and 3 for $V_0 = 4E_R$). In this regime localization effects are due to the nonlinear interactions. The number of atoms in the n th component of a localized state can be calculated as $N_n \sim g_{nn}^{-1} \int \psi_n^2(x) dx$, where g_{nn} is the appropriately scaled 1D nonlinear interaction coefficient. Bright-bright solitons

near the *lower* edges of the first gaps [e.g., at $\mu_{a,b} = 1.96$ in Fig. 2(a)] are widespread and contain a low number of atoms $N_{a,b} \sim 10^2$, in agreement with the experimental observations of single-component gap solitons [9]. Well localized, higher atom number states are found further within the gap [Fig. 2(b)]. The dark-bright composite states near the *upper* edges of the *induced* gaps [see Figs. 3 and 4(a)] are characterized by a wider bright component that can contain an order of magnitude more atoms, $N_b \sim 10^3$, than the near-edge bright-bright gap solitons.

In conclusion, we have shown theoretically that optical lattices can be used to vary *both the type and magnitude* of nonlinear intercomponent interactions in BEC mixtures, and to observe two-component atomic solitons, both in the gaps and bands of the linear Bloch-wave spectrum. The experimental investigation of dark-bright composite states (and their transport properties) within linear spectral bands could be of particular interest.

This work was supported by the Australian Research Council (ARC).

-
- [1] M. Jona-Lasinio *et al.*, Phys. Rev. Lett. **91**, 230406 (2003).
 - [2] M. Cristiani *et al.*, Opt Express **12**, 4 (2004).
 - [3] B. Eiermann *et al.*, Phys. Rev. Lett. **91**, 060402 (2003).
 - [4] L. Fallani *et al.*, Phys. Rev. Lett. **91**, 240405 (2003).
 - [5] E. A. Ostrovskaya and Yu. S. Kivshar, Opt. Express **12**, 19 (2004).
 - [6] For a review, see D. N. Christodoulides, F. Lederer, and Y. Silberberg, Nature (London) **424**, 817 (2003).
 - [7] H. Pu *et al.*, Phys. Rev. A **67**, 43605 (2003).
 - [8] See, e.g., P.J. Louis *et al.*, Phys. Rev. A **67**, 013602 (2003).
 - [9] B. Eiermann *et al.*, cond-mat/0402178.
 - [10] See, e.g., H. Pu and N.P. Bigelow, Phys. Rev. Lett. **80**, 1130 (1998).
 - [11] O. Mandel *et al.*, Phys. Rev. Lett. **91**, 010407 (2003).
 - [12] B. Deconinck *et al.*, J. Phys. A **36**, 5431 (2003).
 - [13] N. A. Kostov *et al.*, cond-mat/0307156.
 - [14] A. A. Sukhorukov and Yu. S. Kivshar, Phys. Rev. Lett. **91**, 113902 (2003).
 - [15] A. S. Desyatnikov *et al.*, Phys. Rev. Lett. **91**, 153902 (2003).
 - [16] A. S. Kovalev and I.V. Gerasimchuk, JETP **95**, 965 (2002).
 - [17] G. Modugno *et al.*, Phys. Rev. Lett. **89**, 190404 (2002).
 - [18] J. H. Denschlag *et al.*, J. Phys. B **35**, 3095 (2002).
 - [19] A. P. Sheppard and Yu. S. Kivshar, Phys. Rev. E **55**, 4773 (1997), and references therein.
 - [20] Yu. S. Kivshar and G. P. Agrawal, *Optical Solitons: From Fibers to Photonic Crystals* (Academic, San Diego, 2003), Chap. 9, and references therein.
 - [21] A.V. Yulin and D.V. Skryabin, Phys. Rev. A **67**, 023611 (2003).
 - [22] Th. Busch and J.R. Anglin, Phys. Rev. Lett. **87**, 010401 (2001).